Title	Experimental and theoretical study of polarization-dependent optical transitions in InAs quantum dots at telecommunication-wavelengths (1300-1500 nm)
Authors	Usman, Muhammad;Heck, Susannah C.;Clarke, Edmund;Spencer, Peter;Ryu, Hoon;Murray, Ray;Klimeck, Gerhard
Publication date	2011
Original Citation	Usman, M., Heck, S., Clarke, E., Spencer, P., Ryu, H., Murray, R. and Klimeck, G. (2011) 'Experimental and theoretical study of polarization-dependent optical transitions in InAs quantum dots at telecommunication-wavelengths (1300-1500 nm)', Journal of Applied Physics, 109(10), 104510 (8pp). doi: 10.1063/1.3587167
Type of publication	Article (peer-reviewed)
Link to publisher's version	http://aip.scitation.org/doi/10.1063/1.3587167 - 10.1063/1.3587167
Rights	© 2011, American Institute of Physics. This article may be downloaded for personal use only. Any other use requires prior permission of the author and AIP Publishing. The following article appeared in Usman, M., Heck, S., Clarke, E., Spencer, P., Ryu, H., Murray, R. and Klimeck, G. (2011) 'Experimental and theoretical study of polarization-dependent optical transitions in InAs quantum dots at telecommunication-wavelengths (1300-1500 nm)', Journal of Applied Physics, 109(10), 104510 (8pp). doi: 10.1063/1.3587167 and may be found at http://aip.scitation.org/doi/10.1063/1.3587167
Download date	2024-04-25 09:17:07
Item downloaded from	https://hdl.handle.net/10468/4738

Experimental and theoretical study of polarization-dependent optical transitions in InAs quantum dots at telecommunication-wavelengths (1300-1500 nm)

Muhammad Usman, Susannah Heck, Edmund Clarke, Peter Spencer, Hoon Ryu, Ray Murray, and Gerhard Klimeck

Experimental and theoretical study of polarization-dependent optical transitions in InAs quantum dots at telecommunication-wavelengths (1300-1500 nm)

Muhammad Usman,[1,a),b)] Susannah Heck,[2] Edmund Clarke,[2,c)] Peter Spencer,[2] Hoon Ryu,[1] Ray Murray,[2] and Gerhard Klimeck[1]

[1]*Network for Computational Nanotechnology, Electrical and Computer Engineering Department, Purdue University, West Lafayette, Indiana 47907, USA*
[2]*Department of Physics, Imperial College London, Blackett Laboratory, Prince Consort Road, London SW7 2AZ, United Kingdom*

The design of some optical devices, such as semiconductor optical amplifiers for telecommunication applications, requires polarization-insensitive optical emission at long wavelengths (1300–1550 nm). Self-assembled InAs/GaAs quantum dots (QDs) typically exhibit ground state optical emissions at wavelengths shorter than 1300 nm with highly polarization-sensitive characteristics, although this can be modified by the use of low growth rates, the incorporation of strain-reducing capping layers, or the growth of closely-stacked QD layers. Exploiting the strain interactions between closely stacked QD layers also affords greater freedom in the choice of growth conditions for the upper layers, so that both a significant extension in their emission wavelength and an improved polarization response can be achieved due to modification of the QD size, strain, and composition. In this paper, we investigate the polarization behavior of single and stacked QD layers using room temperature sub-lasing-threshold electroluminescence and photovoltage measurements, as well as atomistic modeling with the NEMO 3-D simulator. A reduction is observed in the ratio of the transverse electric (TE) to transverse magnetic (TM) optical mode response for a GaAs-capped QD stack as compared to a single QD layer, but when the second layer of the two-layer stack is InGaAs-capped, an increase in the TE/TM ratio is observed, in contrast to recent reports for single QD layers. © *2011 American Institute of Physics*. [doi:10.1063/1.3587167]

I. INTRODUCTION

Single and multiple InAs quantum dot (QD) layers have been explored for their potential use in the implementation of GaAs-based optical devices such as lasers, semiconductor optical amplifiers, and saturable absorber mirrors operating at telecommunication wavelengths (1300–1550 nm).[1–4] The optical properties of QDs are of critical importance because they can be used to control the polarization sensitivity of devices. Several approaches have been explored in order to achieve polarization-insensitive emission from QDs, including covering the QDs with a strain reducing layer,[5] growing multiple electronically coupled layers of QDs[6–8] and columnar QDs,[9,10] and forming a type-II band alignment using GaAsSb barriers.[11] However, to date, there has not been much theoretical guidance available to help people fully understand the optical properties of these QDs. Previous theoretical work[9,12] has explored the properties of columnar QDs using the k•p method, which ignores atomistic granularity. The polarization properties of QDs strongly depend on the ori-

entation of the electron and hole wave functions, which are determined by the asymmetric nature of the interface between the QD and the surrounding GaAs buffer, by strain and piezoelectric fields.[13–15] Any quantitative analysis of QDs must involve modeling and simulations that fully incorporate all of the above mentioned effects. Studies based on continuum methods, such as the effective mass model or k•p,[10,12] lack atomistic resolution and fundamentally cannot include interface roughness, alloy randomness, and strain-induced symmetry lowering, but must resort to average perturbations.

This work explores the wavelength and polarization properties of independent layers (hereafter referred to as single quantum dot (SQD) layers) and two closely stacked layers (bilayers) of InAs/GaAs QDs incorporated into ridge-waveguide laser structures, using room temperature (RT) sub-lasing-threshold electroluminescence (EL) and photovoltage (PV) measurements. The experimental data are analyzed and explained via atomistic modeling of the QD geometries using the NEMO 3-D simulator.[16,17] Our results demonstrate that telecommunication wavelengths can be achieved by growing vertical stacks of independent QDs without incorporating dilute nitride layers or forming columnar QDs. Polarization-resolved measurements and theoretical calculations show a reduction in the ratio of the transverse electric (TE) to transverse magnetic (TM) optical mode response for a GaAs-capped InAs QD bilayer as compared to a single GaAs-capped InAs QD layer.

a)Author to whom correspondence should be addressed. Electronic mail: usman@alumni.purdue.edu.
b)Now at Tyndall National Institute, Lee Maltings Dyke Parade, Cork, Ireland.
c)Now at EPSRC National Centre for III-V Technologies, Centre for Nanoscience and Technology, University of Sheffield, North Campus, Broad Lane, Sheffield S3 7HQ, United Kingdom.

In contrast to a recent study of single InAs QD layers,[5] our experimental and theoretical results indicate an increase in the TE/TM ratio when the upper QD layer in the bilayer is covered by an InGaAs strain-reducing capping layer (SRCL). This increase is due to biaxial strain induced heavy hole (HH)-light hole (LH) splitting, which increases in the presence of an InGaAs SRCL. This result is consistent with our earlier study of single InAs QD layers capped by an InGaAs SRCL.[13] Our experimental measurements and theoretical calculations indicate that an InGaAs SRCL can only redshift the optical wavelength and does not reduce the TE/TM ratio, which is required in order to achieve an isotropic polarization response.

II. EXPERIMENTAL PROCEDURES

The devices investigated here are ridge-waveguide QD laser structures with 500 nm thick GaAs active regions, incorporating a series of three or five QD bilayers, and a reference sample with an active region containing five single QD layers, separated by 50 nm. The active region was surrounded by 1500 nm $Al_{0.3}Ga_{0.7}As$ *n*- and *p*-doped cladding layers. In the SQD sample, each QD layer was grown by annealing the GaAs surface under an As overpressure at 580 °C for 10 min in order to minimize surface undulations before depositing 2.4 ML of InAs at 0.014 ML s^{-1} at 485 °C. The QDs were then capped by 15 nm of GaAs grown at 492 °C, before the remaining 35 nm GaAs cap was grown at 580 °C. These growth conditions yielded QD layers with a QD density of 1.5×10^{10} cm^{-2}. For the GaAs-capped bilayer sample, the first (seed) layer of QDs was formed under conditions similar to those for the SQD sample (2.4 ML of InAs grown at 480 °C with a growth rate of 0.014 MLs^{-1}). These QDs were then capped by a 10 nm GaAs spacer layer, also grown at 480 °C. The sample was then annealed under an As overpressure at 580 °C for 10 min in order to reduce surface undulations and desorb segregated In from the underlying QD layer.[18] The second QD layer was then formed by depositing 3.3 ML of InAs at a lower growth temperature (467 °C). These QDs were then capped by 15 nm of GaAs at 467 °C before the remaining 35 nm GaAs was grown at 580 °C. The reduced growth temperature for the second layer of the bilayer is crucial for achieving the extended emission wavelength and high uniformity of the QDs by suppressing strain-induced intermixing effects.[19,20] The QD density in each layer of the bilayer is 2.7×10^{10} cm^{-2}, similar to the SQD layers. To maximize the emission wavelength, the growth conditions for the InGaAs-capped bilayers were modified and the seed layer was grown at 505 °C, leading to a lower density (5×10^{9} cm^{-2}) of larger QDs. The reduced density and increased size of the QDs in the seed layer lead to a concomitant increase in the size of the QDs in the second layer.[21] The second QD layer was then capped by 4 nm of $In_{0.26}Ga_{0.74}As$ followed by 11 nm of GaAs at 467 °C, before growing the remaining 35 nm of GaAs at 580 °C. These growth conditions lead to an extension of the emission wavelength to 1470 nm at room temperature; this is a shorter wavelength than previously reported for individual InGaAs-capped QD bilayers,[21] but the growth conditions for multiple closely stacked QD bilayers have not yet been optimized. PV measurements were obtained by illuminating the front facet of the devices with either TE- or TM-polarized light from a white light source dispersed by a monochromator.[22]

III. THEORETICAL MODEL

The cross-sectional transmission electron microscopy (TEM) images in Figs. 1(a) and 1(b) indicate that the seed layer QD in our bilayer samples has a diameter of ~20 nm and a height of ~7 nm. The upper QD with a GaAs cap (Fig. 1(a)) has a diameter of ~30 nm and a height of ~8 nm. The InGaAs cap tends to increase the height of the upper QD due to the reduced out-diffusion of indium from the QDs during capping,[20,21,23] resulting in slightly taller QDs with a height of ~10 nm, as can be seen in Fig. 1(b).

Schematics of the model QDs in the SQD and bilayers are shown in Figs. 1(c)–1(e). We consider in Fig. 1(c) an InAs SQD embedded in a GaAs buffer, in Fig. 1(d) a bilayer consisting of two InAs QDs embedded in a GaAs matrix, and in Fig. 1(e) a bilayer consisting of two InAs QDs embedded in a GaAs matrix but with the upper QD capped with a 4 nm $In_{0.26}Ga_{0.74}As$ SRCL. The dimensions of the SQD are same as those of the QDs in the seed layer of the bilayers.

The theoretical calculations are performed using the NEMO 3-D simulator,[16,17] which calculates the electronic structures through multi-million atom simulations based on a 20 band $sp^3d^5s^*$ nearest neighbor empirical tight binding model.[24] Strain is calculated using an atomistic valence force field (VFF) model, with the Keating potential modified to include anharmonic corrections.[25] Both linear and quadratic piezoelectric potentials[14,26] are included. The inter-band optical transition strengths are calculated using Fermi's golden rule as the squared magnitude of the momentum matrix elements summed over the spin degenerate states.[26] We have used large strain domains in order to fully incorporate the long range impacts of strain and piezoelectric fields. For the bilayers, the strain buffer is 70 nm × 70 nm × 66 nm in size, containing approximately 20×10^6 atoms. The strain domain has fixed and free boundary conditions on the bottom and top, respectively, whereas periodic boundary conditions are used in the lateral directions. The electronic domain is relatively small, extending 60 nm laterally and having a height of 50 nm along [001]. We implement closed boundary conditions for the electronic domain in all three dimensions. The passivation of the surface atoms is accounted for according to our published model.[27]

We emphasize here that all simulations are performed using previously published VFF model constants,[28] tight binding parameters,[24] and piezoelectric constants.[29] The only "inputs" into the simulator are the geometries and material compositions indicated in Figs. 1(c)–1(e). The close agreement between the calculations and the experimental results obtained, without adjusting any published parameter, highlights the transferability of the empirical VFF and tight binding parameters, similar to previous work on InAs/GaAs quantum dots[13,26] and SiGe.[30]
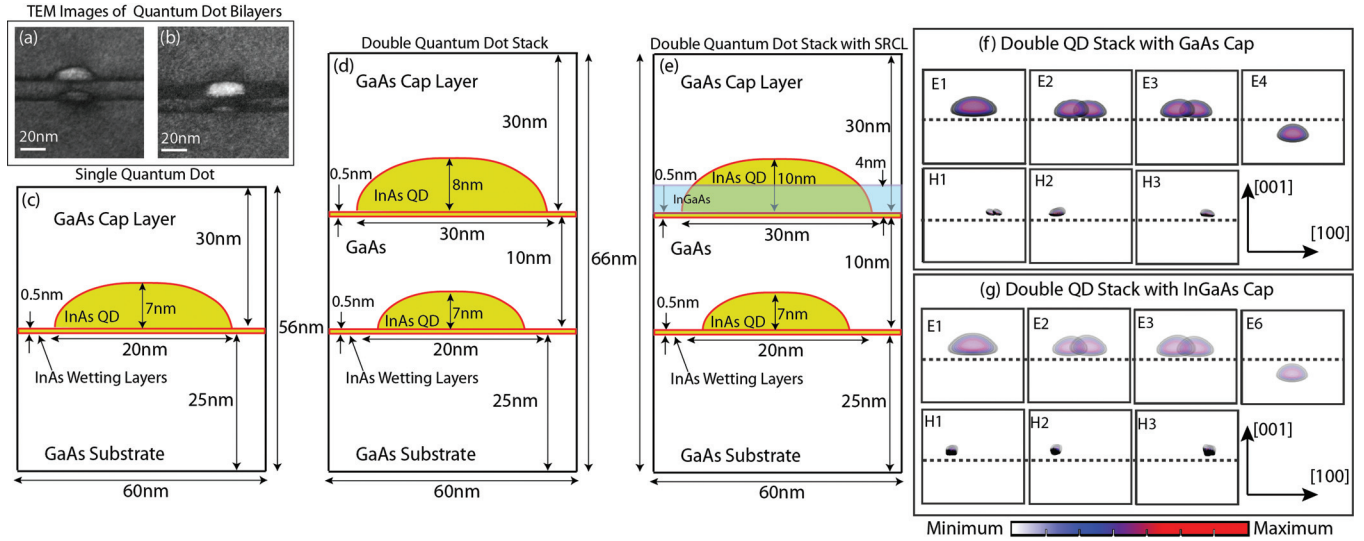
FIG. 1. (Color online) (a, b) TEM Images of the bilayer QD stacks without (a) and with (b) the SRCL capping. The SRCL overgrowth clearly tends to increase the size of the QD. (c) Geometry of a single InAs QD lying on top of a 0.5 nm InAs wetting layer inside GaAs buffer. (d) Geometry of a two InAs QD vertical stack surrounded by GaAs buffer. Both QDs are lying on the top of 0.5 nm wetting layers. The separation between the wetting layers is 10 nm. The upper QD in the stack is larger than the lower QD due to strain-driven self-assembly process. (e) Geometry of a two InAs QD vertical stack surrounded by GaAs buffer. Both QDs are lying on the top of 0.5 nm wetting layers. The separation between the wetting layers is 10 nm. The upper QD is first covered by a 4nm In0.26Ga0.74As strain reducing layer before depositing the GaAs capping layer. The upper QD has slightly larger size than the upper QD of the stack without SRCL (part (d)) due to reduced In segregation effect. (f) Wave function plots of first four electron and first three hole energy levels of the two QD stack (part (e)). The blue and the red colors show the intensity of magnitude (blue is lowest and red is highest). The dotted horizontal line is marked to guide the eyes and separates the upper and the lower QDs. All of the first three electrons and first three holes are in the upper QD indicating that the upper QD is optically active where as the lower QD remain inactive. (g) Wave function plots of four electron and three hole energy levels of the two QD stack with the SRCL cap (part (e)). The first electron state in the lower QD is E6.

IV. RESULTS AND DISCUSSIONS

A. Only the upper QD is optically active

In bilayer QDs, the upper QD is slightly larger than the lower one.[31] Strain due to the upper QD tends to increase the energy of the seed QD energy levels, and thus the lowest electron and highest hole energy levels are confined in the upper QD.[32] Due to a large separation between the QD layers (10 nm), the electron and hole wave functions do not form hybridized molecular states. Such hybridized states can be observed for closely stacked QDs, separated by ∼6 nm or less,[26,32] and they also can be observed by applying an external electric field.[26,33] In both of our bilayers, the first three electron and hole energy levels are confined to the upper QD. The first electron energy level in the lower QD is the fourth energy level, E4, and the sixth energy level, E6, in the GaAs and InGaAs SRCL capped bilayers, respectively. In these bilayers, the upper QD serves as an optically active layer for ground state optical emission. The lower QD does not contribute to optical emission for reasonably low carrier occupation, in agreement with previous photoluminescence (PL) measurements.[20,21,34]

B. Redshift of optical emissions to 1300 nm and beyond

Fig. 2 compares the RT EL spectra obtained from the SQD to that measured on a GaAs capped bilayer. Low current densities (< 25 A cm^{-2}) were used to suppress heating effects and amplify spontaneous emission. The dotted lines are the electron-hole transition energies computed from the NEMO 3-D simulations, which closely match the experimental data. A redshift of ∼77 nm is observed between the SQD and GaAs capped bilayer samples. This is because of the larger height of the upper QD in the bilayer and the strain coupling between the two layers of bilayer, which tend to reduce the optical gap and red shift the optical emission.[32] Figure 2 also compares the RT EL spectra measured on the bilayers with and without the InGaAs-SRCL. An InGaAs-SRCL relaxes the hydrostatic strain and reinforces the biaxial strain, causing a reduction in the optical gap and a further ∼122 nm redshift in the emission wavelength.[13] The short-wavelength peak around 1400 nm observed in the EL spectrum obtained from the InGaAs SRCL bilayer comprises a combination of excited state emissions from the QDs (that are more evident in this spectrum due to the reduced QD density in this sample) and ground state emissions from a population of smaller QDs that are present due to the unoptimized growth conditions. This paper considers only the ground state emission from the main QD population in each sample, so the number of modeled states has not been extended to cover this peak.

C. Physics of the InGaAs-SRCL induced red shifts

In Fig. 3 we compare the local band edges of the lowest conduction band (CB) and the two highest valence bands
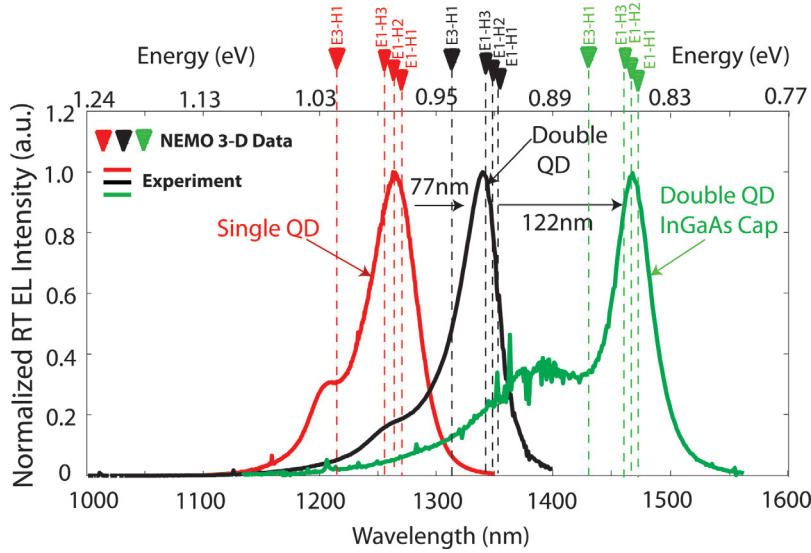
FIG. 2. (Color online) Comparison of the ground state optical emissions from the single InAs QD and the double InAs QD stack without SRCL and with SRCL. The red (single QD), black (QD stack without the SRCL), and green (QD stack with the SRCL) curves show the room temperature electroluminescence spectra measured in the experiment. The vertical dotted lines are the electron-hole transition energies calculated from the NEMO 3-D simulations. A redshift of ~77 nm is observed for the bilayers without the SRCL as compared to the single InAs QDs. The InGaAs SRCL further red shifts the spectrum by ~122 nm. The noise in the green color close to a wavelength of 1400 nm is due to water absorption.

(HH and LH) for the two bilayers (Figs. 1(b) and 1(c)). The InGaAs-SRCL reduces the hydrostatic strain and increases the biaxial strain in the upper QD layer. The CB bandedge therefore shifts to a lower energy while the HH bandedge shifts to a higher energy,[13] resulting in a ~50 meV reduction of the bandgap energy, inducing an ~88 meV change in the optical gap. As a result, the ground state optical emission red

shifts by ~122 nm, and a ground state optical emission at 1470 nm can be achieved.

D. Hole energy levels aligned along (110) and (−110)

Fig. 4 shows a top view of the spatial distribution of the lowest conduction band energy level (E1) and the three highest hole energy levels (H1, H2, and H3) for the SQD sample (top row) and the GaAs capped bilayer (bottom row). E1 possesses a symmetric s-type wave function. However, the hole states are oriented along [110] or [−110], due to strain and piezoelectric field induced symmetry lowering.[13–15,35,36] Figure 4 shows a plot of the wave function for one state corresponding to the Kramer's doublet. The other degenerate state will have a wave function concentrated at the opposite edge of the QD. As mentioned in Sec. III, optical transition rates are calculated by summing the contribution from both degenerate states. It should also be noted that the first three hole wave functions, plotted in Fig. 4, are concentrated at the interface of the QD rather than at the QD center. This is due to the large aspect ratios (height/base) of these QDs, which result in an increase in the biaxial strain at the QD/GaAs matrix interface, creating HH traps (pockets).[35,36]

Due to the anisotropy of the hole wave functions along [110] and [−110], the inter-band optical transitions between the electron and hole states, namely, E1 ↔ H1, E1 ↔ H2, and E1 ↔ H3, will be strongly polarization-dependent. However, polarization-resolved photoluminescence collected from the surface of equivalent unprocessed samples indicates that the emission is isotropic in the plane of the QDs (i.e., TE(110)/TE(−110) ~ 1.0 ± 0.1). An isotropic polarization response has previously been observed in the plane of slightly smaller QDs with a similar aspect ratio (~0.3).[37] The reason for the discrepancy between theory and experiment was unclear, and the authors[37] reported that the anisotropic response might be due to shape variations or possible omissions in the theory.

We demonstrate here that in order to achieve isotropic polarization dependence in the plane of the QDs, more than
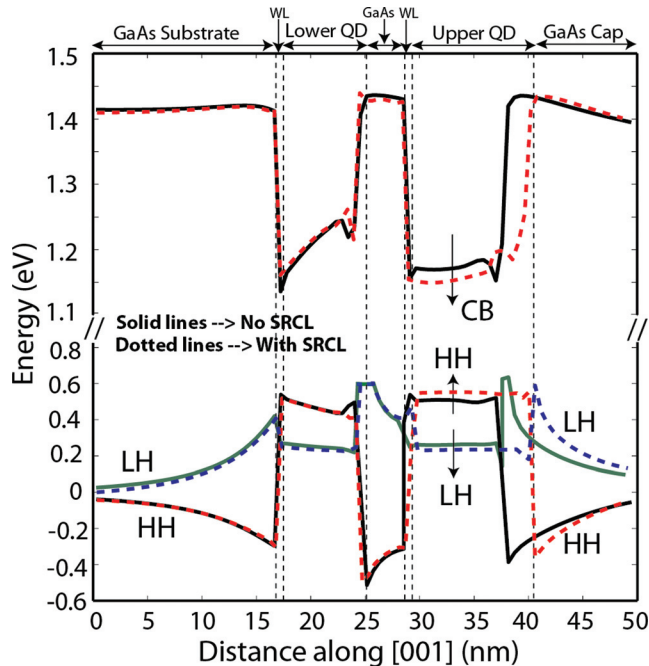

FIG. 3. (Color online) The comparison of the lowest conduction bandedge (CB) and the highest two valence band edges (HH and LH) for the bilayer QD stacks with (dotted lines) and without (solid lines) the SRCL. The InGaAs SRCL shifts the CB to lower energies and the HH bandedge to higher energies, thus reducing the bandgap and increasing the optical emission wavelength. The SRCL also shifts the HH and LH band edges in opposite directions and increases the HH-LH separation. The overall reduction in the bandgap due to the SRCL is ~50 meV and induces a shift of ~88 meV in the optical gap. The shift of the HH band toward higher energies results in an increase in the TE/TM ratio.
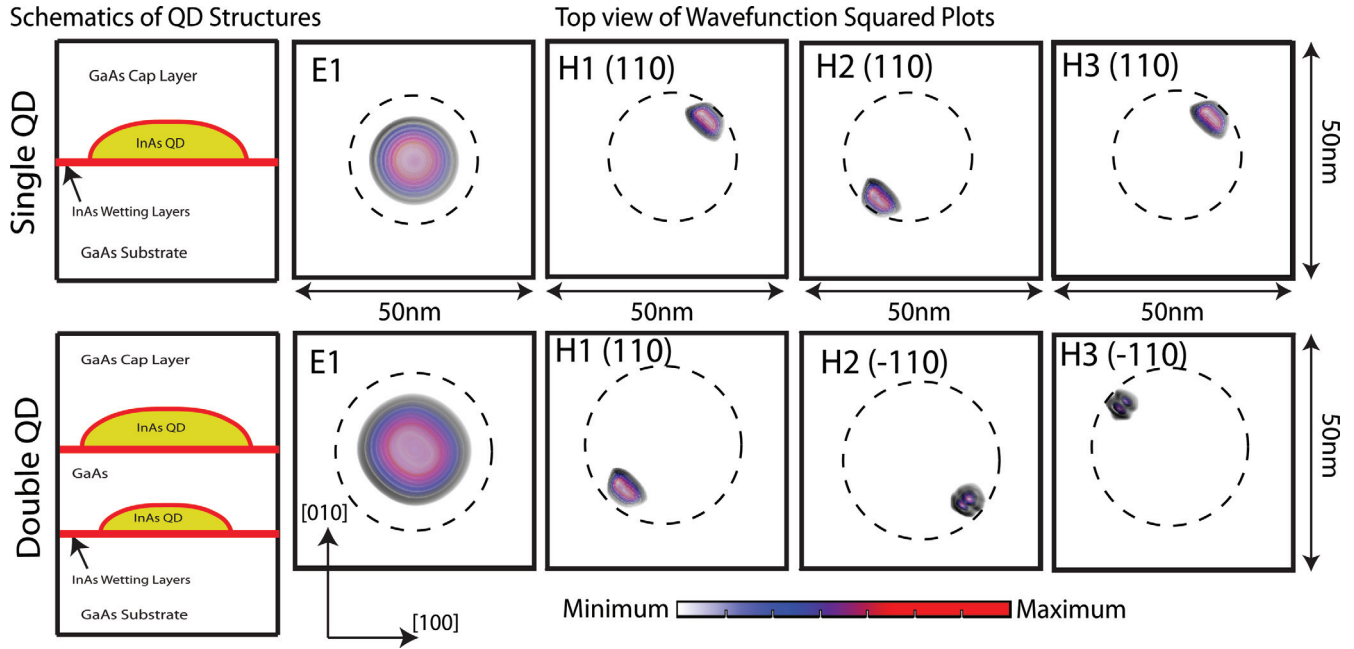
FIG. 4. (Color online) Top view of the wave function plots of the lowest electron energy level (E1) and the three highest hole energy levels (H1, H2, and H3) for the single QD (upper row) and the double QD stack without the SRCL (lower row). The color intensity of the plots indicates the magnitude of the wave function data: the red color corresponds to the maximum value, and the blue color corresponds to the minimum value. Dashed circles are drawn to highlight the boundaries of the QD regions. The leftmost column shows a schematic diagram of the system. The lowest electron energy level is of an s-type character and shows a symmetric distribution of the charge density. The hole energy levels are strongly affected by the strain and piezoelectricity and tend to align along the [110] or [−110] direction.

one hole energy level should be included in the calculation of the ground state optical transition strength. This is because hole energy levels are very closely packed, as can be seen in Fig. 2. The difference between the highest and the lowest transition energies calculated here, (E3-H1) − (E1-H1), is ∼16 meV, ∼12.5 meV, and ∼14 meV for the SQD, the GaAs capped, and the InGaAs SRCL capped bilayer, respectively, indicating that the first three hole energy levels in our QDs are within ∼$0.5k_BT$ (∼ 12.9 meV) at RT. It can therefore be concluded that in our QDs, the topmost valence band states are very closely packed, implying that at RT, multiple hole levels can contribute to the measured transition intensity. In the next section, we show that multiple hole energy levels can indeed simultaneously contribute to the ground state optical emission and thus should be considered in any theoretical calculation of the ground state optical transition strengths.

E. Multiple holes are required in order to achieve isotropic in-plane polarization

Fig. 5 shows the optical intensity computed from the NEMO 3-D simulations as a polar plot for the (a) SQD and (b) GaAs capped bilayer. The direction of the incident light is along [001]. The optical transition intensities are plotted as a function of the angle, θ, measured between [100] and [010]. In Fig. 5(a) we observe a slightly anisotropic polarization dependence (i.e., TE(110)/TE(−110) ∼ 1.18), as the first three hole energy levels are oriented along [110] (top row of Fig. 4), resulting in a slightly weaker TE(−110) mode. Figure 5(b) shows a nearly isotropic polarization

emission for the GaAs-capped bilayer. This is because H1 is oriented along [110], whereas H2 and H3 are both oriented along [−110]. This orthogonal distribution of hole wave functions tends to cancel out the in-plane polarization sensitivity, and thus the resulting optical spectrum becomes nearly polarization insensitive (i.e., TE(110)/TE(−110) ∼ 1.07). We conclude that any theoretical study of the polarization-resolved ground state optical emission should include multiple hole energy levels in order to achieve polarization insensitivity in the plane of the QDs. Previous studies[12,38] considered only the topmost valence band state.

F. TE/TM ratio analysis

For telecommunications applications, a polarization insensitive response is desirable for some edge-emitting devices. Self assembled QDs have low aspect ratios (typically 0.1 to 0.3) and strong carrier confinement along [001], resulting in very anisotropic optical properties, whereby the TE optical mode is dominant and the TM optical mode can be very weak. Large aspect ratio (> 0.6) columnar QDs[9,10] have been designed in order to achieve isotropic in-plane polarization. Here we calculate the polarization dependent optical transitions for our SQD sample and compare it to the response of our GaAs capped and InGaAs SRCL capped bilayers, shown in Figs. 1(c)–1(e). We compare these results to the experimentally measured TE/TM ratios obtained from cleaved-edge PV spectral measurements.
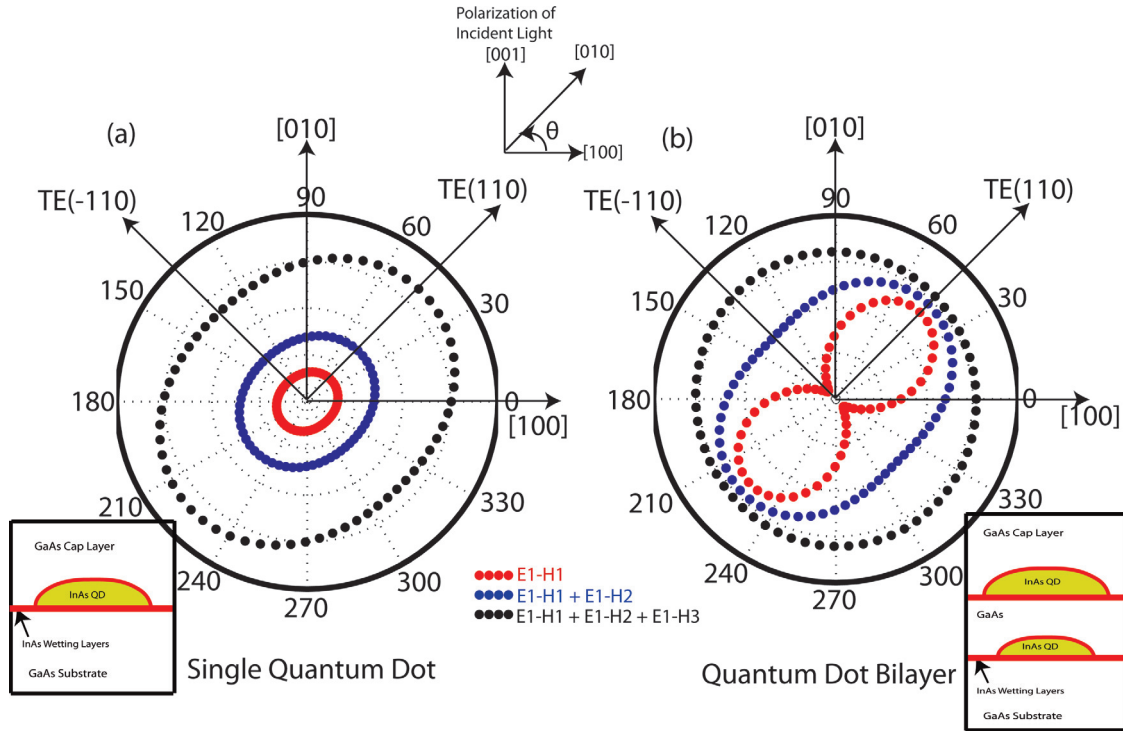
FIG. 5. (Color online) Optical intensity model results represented as polar plots for (a) the single InAs QD and (b) the bilayer InAs QD stack without the SRCL. The schematics of the quantum dot geometry are inserted as insets. The direction of the polarization of the incident light is assumed to be along the [001] direction. The optical transition intensities are plotted as a function of the angle θ between the [100] and the [010] directions. Red dots: only the E1 $\leftrightarrow$ H1 transition is plotted. Blue dots: the sum of the E1 $\leftrightarrow$ H1 and E1 $\leftrightarrow$ H2 transitions is plotted. Black dots: the sum of the E1 $\leftrightarrow$ H1, E1 $\leftrightarrow$ H2, and E1 $\leftrightarrow$ H3 transitions is plotted.

G. SQD to GaAs capped bilayer → TE/TM ratio decreases

Fig. 6 compares the optical intensities computed from the NEMO 3-D simulator and represented as a polar plot for the SQD, the GaAs capped bilayer, and the InGaAs-SRCL capped bilayer. The direction of the incident light is along [−110]. The inter-band optical transition intensities are calculated as a function of the angle θ between [001] and [110], and each curve represents the sum of the optical intensities for E1 $\leftrightarrow$ H1, E1 $\leftrightarrow$ H2, and E1 $\leftrightarrow$ H3. In Fig. 6(a), we see that the TE/TM ratio decreases in going from a SQD to a GaAs capped bilayer, because in a bilayer the strain of the seed QD influences the growth of the upper QD, resulting in a larger upper QD. The taller upper QD reduces the [001] carrier confinement, and thus the TM optical mode is enhanced, leading to a reduction in the TE/TM ratio.

H. GaAs capped bilayer to InGaAs-SRCL capped bilayer → TE/TM ratio increases

Fig. 6(b) compares the polar plots of the bilayer with and without an InGaAs-SRCL. An increase in the polarization sensitivity occurs when the upper QD layer is covered by an InGaAs-SRCL. The reason for this increase can be understood by considering the valence bandedge diagrams in Fig. 3, which show that due to the biaxial strain reinforcement,[13] an InGaAs-SRCL shifts the HH and LH band edges

in opposite directions, leading to an increase in the splitting between the two valence bands. As a result, the topmost valence band states will have an enhanced HH character. We calculate that the HH/LH ratio increases from ~24.41, ~23.23, and ~21.38 to ~25.43, ~23.30, and ~22.19 for H1, H2, and H3, respectively. This increases the TE and suppresses the TM optical mode, resulting in an increase in the TE/TM ratio.

The results for our InGaAs-SRCL capped bilayer are in contrast to those of a recent experimental study[5] in which an InGaAs-SRCL is shown to decrease the TE/TM ratio for a single InAs QD. That result was attributed to the significant increase in the QD aspect ratio, from 0.235 to 0.65, due to the influence of the InGaAs cap in preserving the QD height during the capping process. For our bilayers, the relatively low capping temperature for QDs in the second layer will also preserve the QD height,[20] and we have not observed a significant enhancement in the QD aspect ratio due to the presence of an InGaAs capping layer. The TEM images in Figs. 1(a) and 1(b) clearly indicate that an InGaAs SRCL does not drastically change the aspect ratio of our QDs, in contrast to the InGaAs-capped SQDs reported by Jayavel *et al.*[5]

The table in Fig. 6(c) summarizes the TE/TM ratios from the experimental PV measurements and the NEMO 3-D based calculations for the three QD systems. The calculated values are in reasonable agreement with the experimental measurements for all three cases and show similar trends.
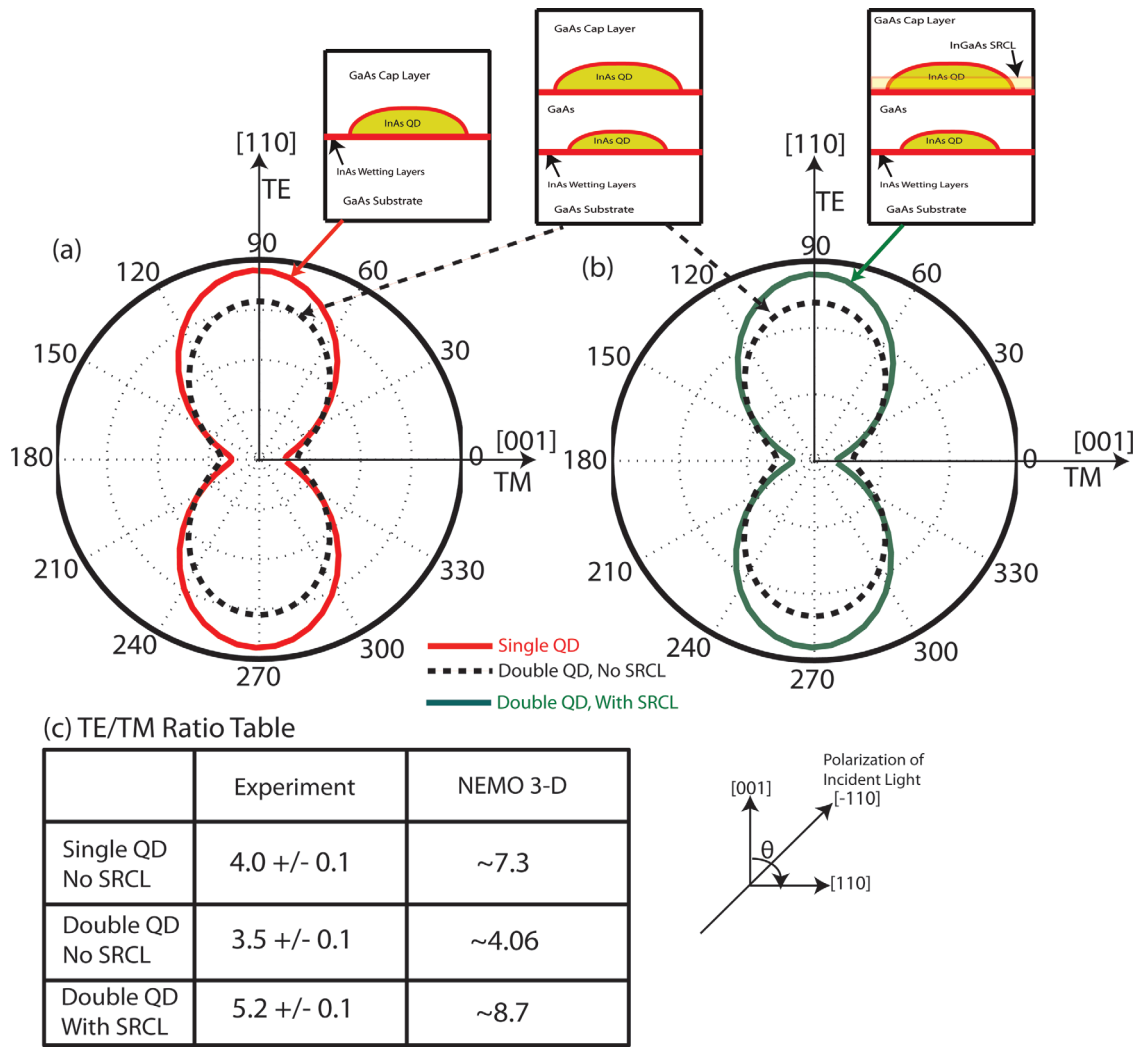
FIG. 6. (Color online) (a), (b) Optical intensity model results represented as polar plots are shown for the single InAs QD (red solid curve), the bilayer InAs QD stack without SRCL (black dotted curve), and the bilayer InAs QD stack with SRCL (green solid line). The schematics of the quantum dot geometry are inserted as small insets. The direction of the polarization of the incident light is assumed to be along the [−110] direction. The inter-band optical transition intensities are calculated as a function of the angle θ between the [110] and the [001] directions. Each curve represents the sum of the intensities of the E1 ↔ H1, E1 ↔ H2, and E1 ↔ H3 transitions. (c) The comparison of the TE(110)/TM(001) ratios for the three QD systems from experimental PV measurements and NEMO 3-D calculations.

V. CONCLUSIONS

We have experimentally and theoretically investigated the RT optical properties of single InAs/GaAs QD layers and InAs/GaAs QD bilayers. Ground state optical emission at wavelengths in excess of 1300 nm is achieved using QD bilayers. PV measurements and optical transition strength calculations indicate reduced polarization sensitivity for the GaAs capped bilayers, as compared to our SQDs. However, an InGaAs-SRCL increases the polarization dependence due to biaxial strain enhancement. This is in contrast to a recent experimental study[5] in which an InGaAs-SRCL is shown to reduce the polarization sensitivity of independent QD layers. A comparison of the results of the calculations with surface PL measurements indicates that more than one hole energy level must be included in the calculation of ground state optical spectra in order to achieve the experimentally measured isotropic polarization sensitivity in the plane of the QDs. Atomistic strain, piezoelectricity, electronic structure, and opti-

cal transition strength calculations are in reasonable agreement with the experimental measurements and help one to understand the optical properties of such QD systems.

Institute) and Professor Timothy B. Boykin (University of Alabama) about the calculation of HH and LH contributions in the valence band states.

[1]D. L. Huffaker, G. Park, Z. Zou, O. B. Shchekin, and D. G. Deppe, Appl. Phys. Lett. **73**, 2564 (1998).

[2]N. N. Ledentsov, A. R. Kovsh, A. E. Zhukov, N. A. Maleev, S. S. Mikhrin, A. P. Vasil'ev, E. S. Semenova, M. V. Maximov, Yu. M. Shernyakov, N. V. Kryzhanovskaya, V. M. Ustinov, and D. Bimberg, Electron. Lett. **39**, 1126 (2003).

[3]S. Dommers, V. V. Temnov, U. Woggon, J. Gomis, J. Martinez-Pastor, M. Laemmlin, and D. Bimberg, Appl. Phys. Lett. **90**, 033508 (2007).

[4]M. P. Lumb, P. N. Stavrinou, E. M. Clarke, R. Murray, C. G. Leburn, C. Jappy, N. K. Metzger, C. T. A. Brown, and W. Sibbett, Appl. Phys. B **97**, 53 (2009).

[5]P. Jayavel, H. Tanaka, T. Kita, O. Wada, H. Ebe, M. Sugawara, J. Tatebayashi, Y. Arakawa, Y. Nakata, and T. Akiyama, Appl. Phys. Lett. **84**, 1820 (2004).

[6]P. Yu, W. Langbein, K. Leosson, J. M. Hvam, N. N. Ledentsov, D. Bimberg, V. M. Ustinov, A. Yu. Egorov, A. E. Zhukov, A. F. Tsatsul'nikov, and Yu. G. Musikhin, Phys. Rev. B **60**, 16680 (1999).

[7]T. Inoue, M. Asada, N. Yasuoka, O. Kojima, T. Kita, and O. Wada, Appl. Phys. Lett. **96**, 211906 (2010).

[8]L. Fortunato, M. T. Todaro, V. Tasco, M. De Giorgi, M. De Vittorio, R. Cingolani, and A. Passaseo, Superlattices Microstruct. **74**, 72 (2010).

[9]P. Ridha, L. Li, M. Rossetti, G. Patriarche, and A. Fiore, Opt. Quantum Electron. **40**, 239 (2008).

[10]J. Andrzejewski, G. Sęk, E. O'Reilly, A. Fiore, and J. Misiewicz, J. Appl. Phys. **107**, 073509 (2010).

[11]T. T. Chen, C. L. Cheng, Y. F. Chen, F. Y. Chang, H. H. Lin, C. T. Wu, and C. H. Chen, Phys. Rev. B **75**, 033310 (2007).

[12]T. Saito, H. Ebe, Y. Arakawa, T. Kakitsuka, and M. Sugawara, Phys. Rev. B **77**, 195318 (2008).

[13]M. Usman, H. Ryu, I. Woo, D. S. Ebert, and G. Klimeck, IEEE Trans. Nano. **8**, 330 (2009).

[14]A. Schliwa, M. Winkelnkemper, and D. Bimberg, Phys. Rev. B **76**, 205324 (2007).

[15]S. Ahmed, M. Usman, N. Kharche, A. Schliwa, and G. Klimeck, in *Proceedings of the 2nd International Conference on Nano/Micro Engineered and Molecular Systems (NEMS)* (IEEE, New York, 2007), pp. 937–942.

[16]G. Klimeck, S. S. Ahmed, B. Hansang, N. Kharche, S. Clark, B. Haley, L. Sunhee, M. Naumov, R. Hoon, F. Saied, M. Prada, M. Korkusinski, T. B. Boykin, R. Rahman, IEEE Trans. Electron Devices **54**, 2079 (2007).

[17]G. Klimeck, S. S. Ahmed, N. Kharche, M. Korkusinski, M. Usman, M. Prada, and T. B. Boykin, IEEE Trans. Electron Devices **54**, 2090 (2007).

[18]P. Howe, E. C. Le Ru, E. Clarke, R. Murray, and T. S. Jones, J. Appl. Phys. **98**, 113511 (2005).

[19]M. O. Lipinski, H. Schuler, O. G. Schmidt, K. Eberl, and N. Y. Jin-Phillipp, Appl. Phys. Lett. **77**, 1789 (2000).

[20]E. C. Le Ru, P. Howe, T. S. Jones, and R. Murray, Phys. Rev. B **67**, 165303 (2003).

[21]E. Clarke, P. Howe, M. Taylor, P. Spencer, E. Harbord, R. Murray, S. Kadkhodazadeh, D. W. McComb, B. J. Stevens, and R. A. Hogg, J. Appl. Phys. **107**, 113502 (2010).

[22]S. C. Heck, S. Osborne, S. B. Healy, E. P. O'Reilly, F. Lelarge, F. Poingt, O. Le Gouezigou, and A. Accard, IEEE J. Quantum Electron. **45**, 1508 (2009).

[23]Ch. Heyn and W. Hansen, J. Cryst. Growth **251**, 140 (2003).

[24]T. B. Boykin, G. Klimeck, R. C. Bowen, and F. Oyafuso, Phys. Rev. B **66**, 125207 (2002).

[25]O. L. Lazarenkova, P. von Allmen, F. Oyafuso, S. Lee, and G. Klimeck, Appl. Phys. Lett. **85**, 4193 (2004).

[26]M. Usman, Y. H. Tan, H. Ryu, S. Ahmed, T. B. Boykin, and G. Klimeck, "Quantitative excited state spectroscopy of a single InGaAs quantum dot molecule through multi-million atom electronic structure calculations," e-print arXiv: 1008.3127v1.

[27]S. Lee, J. Kim, L. Jönsson, J. W. Wilkins, G. W. Bryant, and G. Klimeck, Phys. Rev. B **66**, 235307 (2002).

[28]P. Keating, Phys. Rev. **145**, 737 (1966).

[29]A. Schliwa, M. Winkelnkemper, and D. Bimberg, Phys. Rev. B **76**, 205324 (2007).

[30]N. Kharche, M. Prada, T. B. Boykin, and G. Klimeck, Appl. Phys. Lett. **90**, 092109 (2007).

[31]Q. Xie, A. Madhukar, P. Chen, and N. P. Kobayashi, Phys. Rev. Lett. **75**, 2542 (1995).

[32]M. Usman, S. Ahmed, and G. Klimeck, in *Proceedings of the 8th IEEE Conference on Nanotechnology* (IEEE, New York, 2008), pp. 541–544.

[33]H. J. Krenner, M. Sabathil, E. C. Clark, A. Kress, D. Schuh, M. Bichler, G. Abstreiter, and J. J. Finley, Phys. Rev. Lett. **94**, 057402 (2005).

[34]P. Howe, E. C. Le Ru, E. Clarke, B. Abbey, R. Murray, and T. S. Jones, J. Appl. Phys. **95**, 2998 (2004).

[35]L. He, B. Bester, and A. Zunger, Phys. Rev. B **70**, 235316 (2004).

[36]G. A. Narvaez, G. Bester, and A. Zunger, J. Appl. Phys. **98**, 043708 (2005).

[37]P. W. Fry, M. S. Skolnick, D. J. Mowbray, I. E. Itskevich, J. J. Finley, L. R. Wilson, K. L. Schumacher, J. A. Barker, E. P. O'Reilly, M. Al-Khafaji, A. G. Cullis, M. Hopkinson, J. C. Clark, and G. Hill, Physica E (Amsterdam) **9**, 106 (2001).

[38]W. Sheng and J. P. Leburton, Appl. Phys. Lett. **80**, 2755 (2002).